

# Cross correlation method for PFN investigation

O.V. Zeynalova <sup>a,b</sup>, Sh. Zeynalov <sup>a</sup>

<sup>a</sup>Joint Institute for Nuclear Research, Dubna, Russia

<sup>b</sup>Moscow State Institute of Radioengineering, Electronics and Automation, Moscow, Russia

**Abstract.** Do the prompt neutron emission in spontaneous fission of  $^{252}\text{Cf}$  has been investigated applying cross correlation method and digital signal processing algorithms. A new mathematical approach for neutron/gamma pulse shape separation was developed and implemented for prompt fission neutron (PFN) time-of-flight measurement. The main goal was development of automated data analysis algorithms and procedures for data analysis with minimum human intervention. Experimental data was taken with a twin Frisch-grid ionization chamber and a NE213-equivalent neutron detector in an experimental setup similar to well work of C. Budtz- Jorgensen and H.-H. Knitter [1]. About  $2 \cdot 10^7$  fission events were registered with  $2 \cdot 10^5$  neutron/gamma detection in coincidence with fission fragments. Fission fragment kinetic energy, mass and angular distribution, neutron time-of-flight and pulse shape have been investigated using a 12 bit waveform digitizer not replace the word “abstract,” but do replace the rest of this text. If you must insert a hard line break, please use Shift+Enter rather than just tapping your "Enter" key. You may want to print this page and refer to it as a style sample before you begin working on your paper.

**Keywords:** spontaneous fission,  $^{252}\text{Cf}$ , prompt fission neutron emission, neutron multiplicity, fission fragment mass distribution, total kinetic energy distribution.

**PACS:** 24.75.+i; 25.85.Ca; 28.20.-v; 29.40.Cs; 29.85.Fj.

## INTRODUCTION

Nuclear fission model and prompt fission neutron emission (PFN) was first developed by N. Bohr and J. Wheeler, where nuclei considered as a drop of charged liquid, which surface constantly distorted in competition between attractive nuclear and repulsive Coulomb forces. Rarely large distortion brought the nuclear into the configuration, where repulsion could not be compensated by nuclear force and the system split, sometimes after neutron emission. In this case the neutrons, called scission neutrons in order to distinguish them from the PFN, which are emitted from the fully accelerated fission fragments. The configuration of nuclear shape just before split can be monitored experimentally by measurement of fission fragment (FF) kinetic energy release along with PFN velocity and the angle between fission axis and PFN measurement in single fission event. In new experimental approach developed in ref. [1] authors investigated PFN emission in spontaneous fission of  $^{252}\text{Cf}$  using twin Frisch-grid ionization chamber (TIC) for FF kinetic energies and PFN emission angle along with PFN velocity measurement with help of liquid scintillator (NE213) based neutron detector (ND). Despite the authors demonstrated a power and high capacity of the new approach, some of their results (dependence of average PFN multiplicity on FF total kinetic energy) could not be understood from analysis of the energy balance in fission. The main efforts undertaken recently was development of the experimental technique, using modern

digital pulse processing (DPP), implemented with the detector signals along with in depth mathematical analysis of experimental data.

### EXPERIMENTAL SETUP AND DPP FOR FF SPECTROSCOPY

A sketch of the experimental setup with digital pulse processing electronics is shown in Fig. 1. A TIC was used for fission fragment mass-TKE and PFN emission angle ( $\Theta$ ) measurement. A target with fissile material, deposited on thin nickel foil located on the common cathode of the chamber. Fission fragments were decelerated inside sensitive volume of two independent chambers spending their kinetic energy for free electron creation. Free electrons drifted inside the chamber to respective anodes. The electric charge, induced on two anodes and common cathode were proportional to fission fragments kinetic energy, are measured by three synchronized waveform digitizers (WFD). Approximately 0.15% of fission fragment detection coincided with neutron detection by ND, which signal was digitized using fourth WFD. The common time base was achieved due to all four digitizer sampled detector pulses synchronously and the common cathode pulse was considered as an indication of a fission event. The common cathode pulse was used as a “T-zero” signal for PFN time-of-flight measurement and as one of the input pulses of coincidence unit. A neutron detected inside the

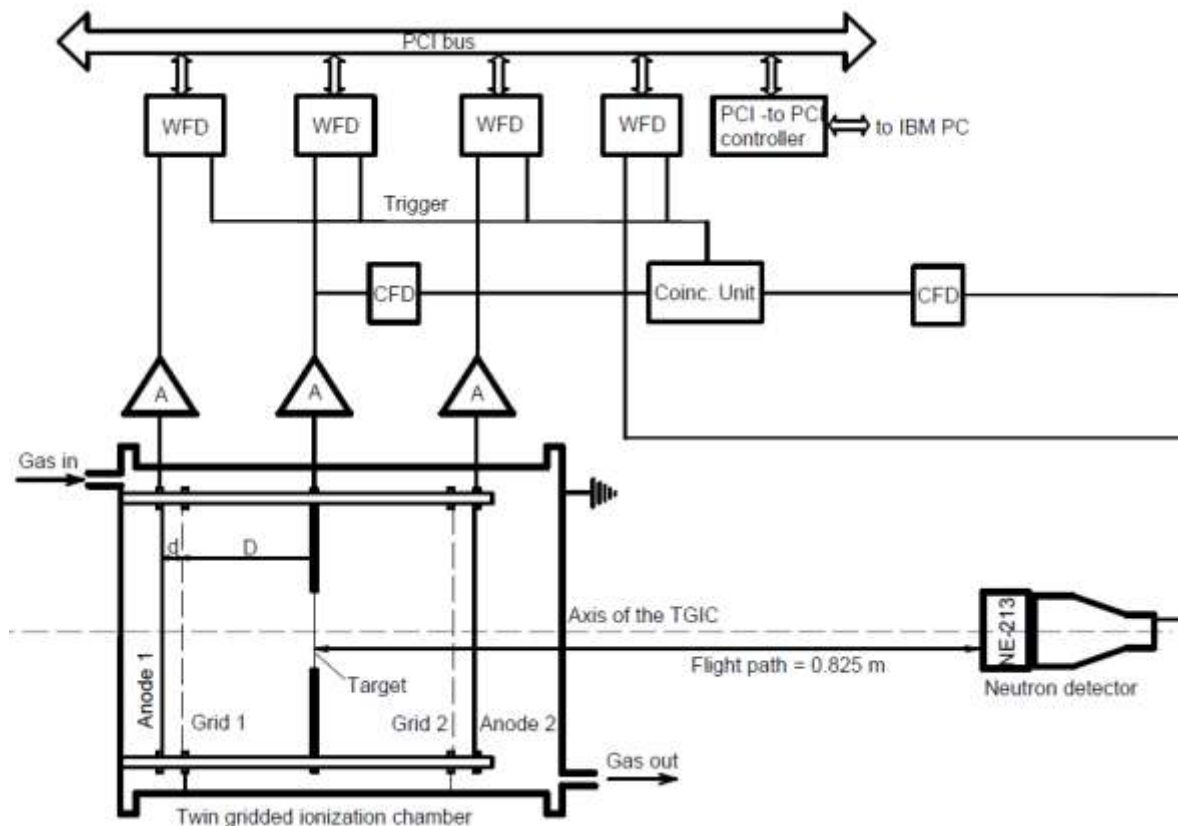
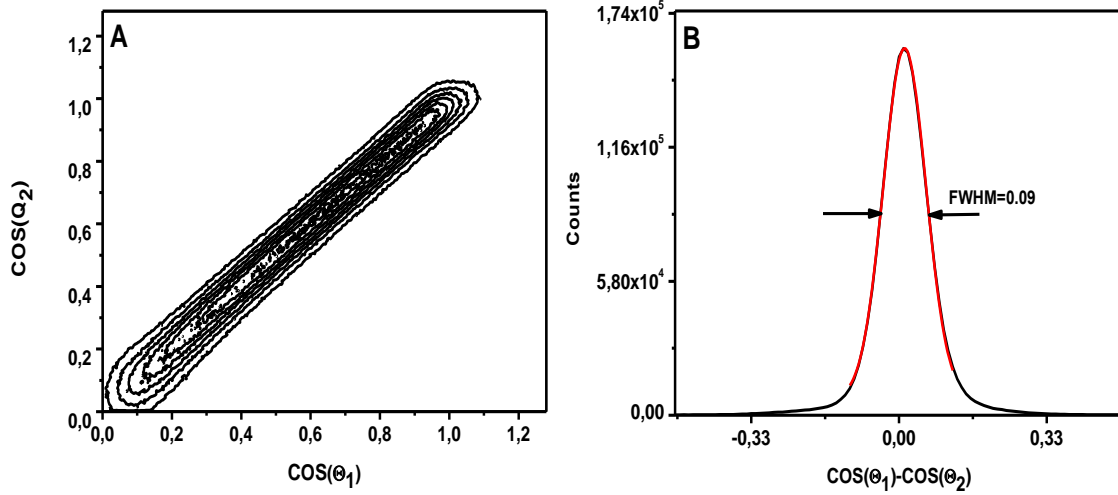


FIGURE 1. Sketch of experimental setup.

time interval of 200 ns duration after “T-zero” was considered as PFN. In such a way two types of fission events were recorded in given experiment: with and without coincidence with ND pulse.



**FIGURE 2.** A) Two dimensional plot in coordinates  $[\text{COS}(\Theta_1), \text{COS}(\Theta_2)]$ . B) Statistical errors distribution in  $\text{COS}(\Theta)$  measurement demonstrating precision of cosine measurement in the range  $\text{cos}(\Theta) > 0.5$ .

Apparently, the intensity of fission events coinciding with ND was proportional to conditional probability of neutron emission in a detected fission event. In given experiment the following parameters of fission event were required to be measured: kinetic energies of correlated FF, their angle in respect to the TIC axis, PFN time-of-flight and the angle between FF and PFN (thanks to allocation of ND on the TIC axis). The information about listed parameters was retrieved from the sampled TIC and ND pulses using DPP algorithms. The waveform of the anode signal, being preprocessed by charge-sensitive preamplifier, was step-like pulse with height proportional to total charge of the electrons released during FF deceleration. The FF angle information can be obtained from the anode pulse rise time, which was proportional to the electron drift time from the point of origin to the respective anode. Fig. 2 demonstrates precision of cosine measurement in whole range (fig. 2A) and in the range of  $\text{cos}(\Theta) = 0.5 * (\text{cos}(\Theta_1) + \text{cos}(\Theta_2)) \geq 0.5$  (fig. 2B).

Charge induced on the anode when free electrons with total charge  $q$  are drifting from the point of origin  $x$  (we suppose the  $x$ -axis aligned along the FF motion direction) to a point of absorption at the anode surface can be calculated using the following formula [2]:

$$Q(D+d) = \int_0^L e\rho(x) \left(1 - \sigma \frac{x \cos(\Theta)}{D}\right) dx = Ne \left(1 - \sigma \frac{\bar{X} \cos(\Theta)}{D}\right). \quad 1$$

In eq. 1 the  $\bar{X} = \int_0^L x\rho(x)dx$  is the “centre of charge” and  $N = \int_0^L \rho(x)dx$  is a total number of electrons, created during the FF deceleration. Drift time  $T$  of the “charge centre” of FF ionization from the point of origin to the point with coordinate  $y = D + \frac{l}{2}$  could be calculated as:

$$T = \frac{D}{W} \left(1 + \frac{l}{2D} - \frac{\bar{X}}{D} \cos(\Theta)\right). \quad 2$$

Eq. 2 describes dependence of  $\cos(\theta)$  on the drift time  $T$ . The DPP algorithms and practical implementation of pulse height and angle evaluation were described in previous papers [3, 4]. In the next chapter we provided description of our approach to PFN time-of-flight spectroscopy.

## TOF AND PFN KINETIC ENERGY EVALUATION

Measurement of PFN time-of-flight in present experiment was done using cathode pulse of TIC as a “T-zero” signal and the ND signal as “Stop” signal. Time difference between these two signals was considered as the PFN time-of-flight (TOF). Narrow

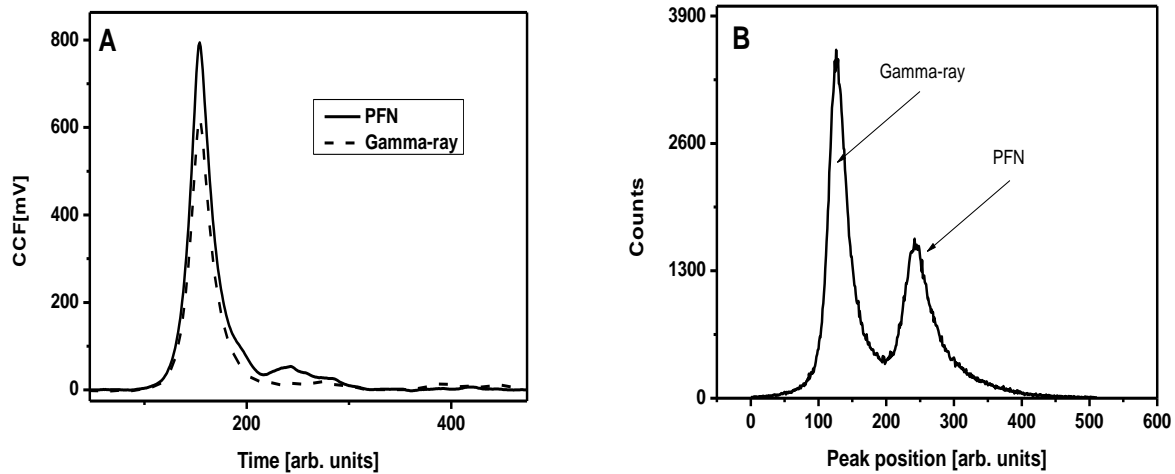


**FIGURE 3.** A) CCF calculated for PFN and fission gamma-ray. B) Distribution of CCF’s “centre-of-gravity” obtained from the experimental data using eq. 5. Two peaks are corresponded to different pulse shapes as indicated on the plot.

bandwidth (100 MHz sampling) available in our measurements and wide pulse height range ( $\sim 100$ ) of ND pulses, made data analysis more complicated due to some surprising effects was not foreseen beforehand. ND, used in experiment, was sensitive to prompt fission gamma radiation and this fact became helpful to overcome the limitation of narrow bandwidth of the apparatus. The bandwidth of ND pulse can be evaluated from the pulse rise time, which was found to be  $\sim 100$  MHz for  $\sim 4$  ns rise time. Because of 100 MHz sampling frequency and taking into account Shannon sampling theorem the signal bandwidth was limited with help of anti-aliasing filter of 4-th order (Bessel filter with 45 MHz cutoff frequency). Constant fraction time triggering (CFTT) was implemented digitally to measure the time difference between TIC cathode and ND pulses. Additionally the TIC cathode pulse before CFTT was preprocessed using “differentiating” procedure realized by subtracting the waveform obtained by passing the original waveform through a second order low pass filter from the original waveform. The latest procedure was linear and guaranteed base line shift compensation. Constant fraction value was selected 0.1 of pulse height and parabolic interpolation was implemented between successive samples. In our data analysis procedure two types of neutron/gamma separation algorithms were implemented. First one was based on integrating of ND current pulse over two different time periods (TII) [4-5]. The second one is based on cross-correlation of the ND waveform ( $ND(t)$ ) with the analytical function, obtained by fit of ND response to fission gamma-radiation according to the following formula:

$$R(t) = A * (1 - \exp(-t/T_1)) * \exp(-t/T_2), \quad 3$$

where  $A, T_1, T_2$  were fitting parameters. The cross-correlation function (CCF) was calculated according to formula:

$$CCF(k * \Delta) = \sum_i R(i * \Delta) ND((k + i) * \Delta), \quad 4$$

where functions  $CCF(t)$ ,  $R(t)$  and  $ND(t)$  were sampled in homogeneously distributed intervals of width  $\Delta$  and  $k, i$  are indexes running from 0 to  $N - 1$  – total number of waveform samples. CCF was calculated event by event and its “centre-of-gravity” value- $G$ , calculated according to eq. 5 was considered as neutron/gamma separation criterion. When the “centre-of-gravity” was located to the right from the deep of distribution from fig. 4B, then the waveform was considered to be belonging to PFN, otherwise the waveform was caused by fission gamma-ray.

$$G = \frac{\sum_i i * CCF(i * \Delta)}{\sum_i CCF(i * \Delta)}. \quad 5$$

Typical CCF calculated using eq. 4 for PFN and fission gamma-ray demonstrated on fig. 3B. Comparison of two criterions was demonstrated on fig. 4B. It is clear that CCF criterion

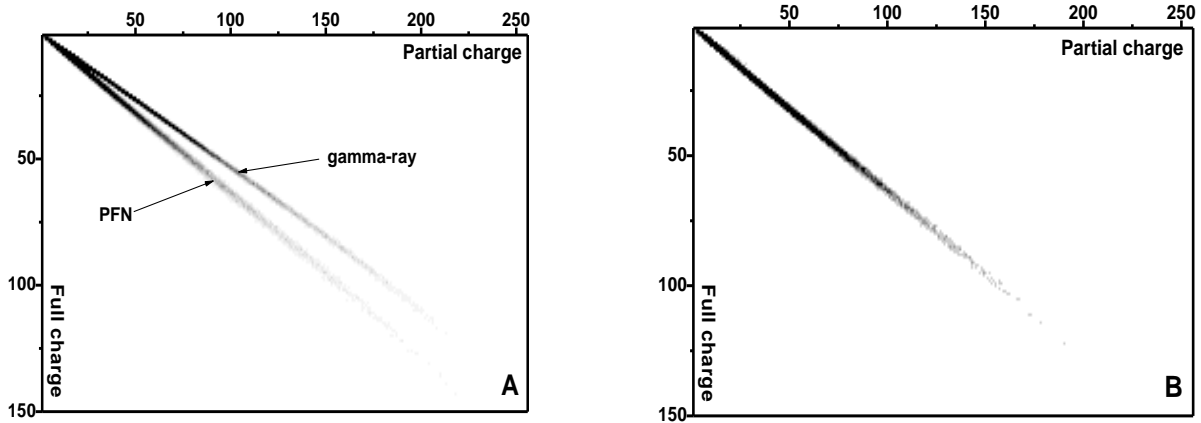


**FIGURE 4.** A) Two dimensional plot in coordinates TOF – total charge (the value obtained when ND signal integrated over the interval, covering full duration of the ND pulse), with CCF neutron/gamma separation criterion. B) Comparison of TOF distribution obtained by integration of distribution from fig. 4A over total charge with similar distribution for two interval criterion.

produced pretty good neutron/gamma separation. To achieve almost similar quality of neutron/gamma separation in our previous work [6] in addition to TII criterion the threshold in ND signal, depending on the total charge was implemented. The data analysis procedure was developed, where broadening of “gamma-peak” in TOF distribution (time resolution) has been taken into account. The broadening of the “gamma-peak” was parameterized as a function of total charge, the similar dependence was supposed for PFN.

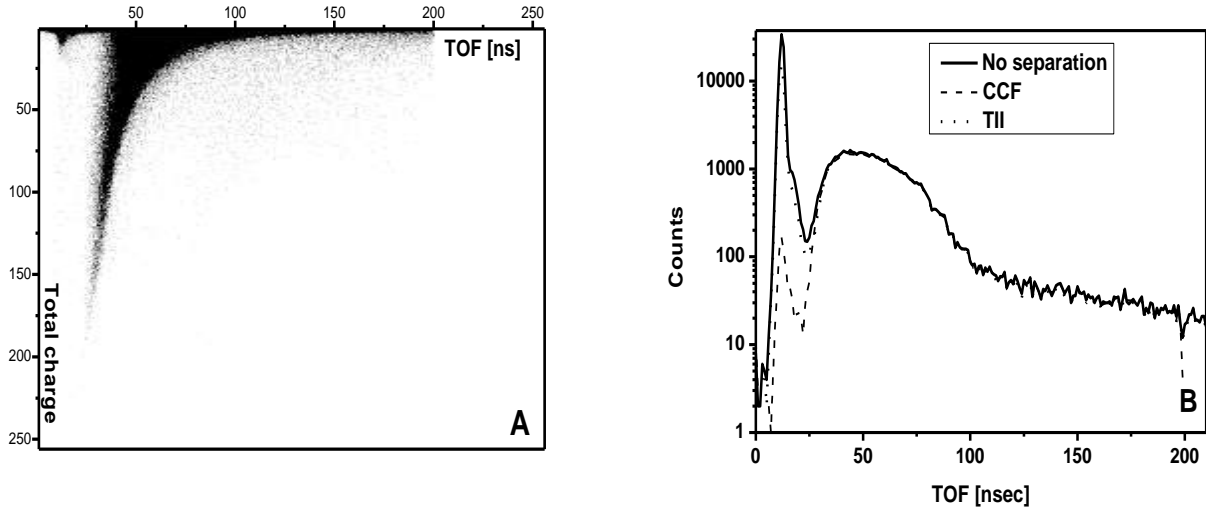


**FIGURE 5.** A) Two-dimensional scatter plot, obtained from experimental data demonstrating TII criterion for neutron/gamma separation. B) The same plot as in A), but plotted only for events having CCF “centre of gravity” parameter greater than parameter from fig. 3B.

Relation between the measured –  $t$  and the actual -  $\tau$  TOF values was deduced from the following equation:

$$p(t) = \int_0^{\infty} \varepsilon(\tau) s(\tau) h(t - \tau) d\tau, \quad 6$$

where  $p(t)$  is the measured TOF distribution  $h(t - \tau)$  is the response function,  $\varepsilon(\tau)$  - ND efficiency function and  $s(\tau)$  is the Maxwell distribution with temperature parameter 1.42 MeV.

Eq. 6 can be resolved in respect to the product  $\varepsilon(\tau) \cdot s(\tau)$ , if  $h(t - \tau)$  is known. Then one can easily find the efficiency function  $\varepsilon(\tau)$  as described in ref. [6].

After DPP application to fission event the following information was recorded: two correlated FF pulse heights along with the FF angle information, the “T-zero”, the TOF value and a pulse shape information. Pulse shape information was given by the values of CCF “gravity centre” position, two ND charge integrals, obtained by integrating ND signal over time interval covering only the leading edge area and full coverage of ND signal. Fig. 5A demonstrates two-dimensional distribution, where coordinates are charge integrals over short and long time periods. To demonstrate the quality of neutron/gamma separation in fig. 5B the same distribution is plotted after applying the CCF criterion.

In summary of description of data analysis procedure described above the following important goal was achieved: our analysis guarantees low background from fission gamma-radiation, it takes correctly into account dependence of response function in Eq. 6 from ND signal (presuming the same shape of response function for PFN as for fission gamma-radiation), our data analysis relies on the Maxwell shape of PFN energy spectrum.

## DISCUSSION

Application of mathematical analysis of signal formation in TIC and developed DPP algorithms for prompt fission neutron TOF spectroscopy allowed us to avoid some uncertainties and correct the final results of PFN emission investigation using new full digital approach to data acquisition and data analysis. Thanks to digitization we implemented new fully digital neutron/gamma separation algorithm allowing effective separation of PFN from prompt gamma-rays.

## ACKNOWLEDGMENTS

This work partially was supported by RFBR grant 10-07-00541-a.

## REFERENCES

1. C. Budtz-Jørgensen and H.-H. Knitter , *Nucl. Phys.*, **A490**, 307(1988).
2. O. Zeynalova, Sh. Zeynalov, M. Nazarenko, F.J. Hamsch, and S. Oberstedt, AIP Conf. Proc. 1404, 325 (2011).
3. O. Zeynalova, Sh. Zeynalov, F.-J. Hamsch and S. Oberstedt, “DSP Algorithms for Fission Fragment and Prompt Fission Neutron Spectroscopy in *Application of Mathematics in Technical and Natural Sciences-2010*, edited by M.D. Todorov and C.I. Christov, AIP Conference Proceedings 1301, American Institute of Physics, Melville, NY, 2010, pp. 430-439.
4. O.V. Zeynalova, Sh.S. Zeynalov, F.-J. Hamsch, S. Oberstedt, *Bulletin of Russian Academy of Science: Physics*, 73, 506-514 (2009).
5. O. Zeynalova, Sh. Zeynalov , F.-J. Hamsch, S. Oberstedt and I. Fabry, “DSP Algorithms for Fission Fragment and Prompt Fission Neutron Spectroscopy in *Application of Mathematics in Technical and Natural Sciences-2010*, edited by M. D. Todorov and C. I. Christov, AIP Conference Proceedings 1186, American Institute of Physics, Melville, NY, 2009, pp. 156-163.
6. Sh. Zeynalov, O.V. Zeynalova, F.-J. Hamsch, S. Oberstedt, *Physics Procedia* Volume 31, 2012, pp 132–140.